IEEE Access
Multidisciplinary | Rapid Review | Open Access Journal

Received September 22, 2019, accepted October 8, 2019, date of publication October 11, 2019, date of current version October 24, 2019.

Digital Object Identifier 10.1109/ACCESS.2019.2946960

Nonlinearity-Based Single-Channel Monopulse Tracking Method for OFDM-Aided UAV A2G Communications

XI PAN[1], CHAOXING YAN[2], (Member, IEEE), AND JIANKANG ZHANG[3], (Senior Member, IEEE)

[1]School of Mechatronical Engineering, Beijing Institute of Technology, Beijing 100081, China
[2]Beijing Research Institute of Telemetry, Beijing 100076, China
[3]Department of Electronics and Computer Science, University of Southampton, Southampton SO17 1BJ, U.K.

Corresponding author: Chaoxing Yan (chaoxing@bit.edu.cn)

This work was supported by the National Natural Science Foundation of China under Grant U1730109 and Grant 61571401.

ABSTRACT Unmanned aerial vehicles (UAVs) have attracted great interest in rapid deployment for both civilian and military applications. The conventional UAV monopulse tracking technique requires dedicated pulses which suffer from multipath effect in air-to-ground (A2G) link with low elevation angles, whereas the orthogonal frequency division multiplexing (OFDM) for A2G high rate communication under frequency selective fading channel was not yet investigated for UAV target tracking at ground station. In this paper, we propose a single-channel monopulse tracking (SCMT) angle estimation method in OFDM tracking receiver exploiting square- and absolute-value nonlinear detection of amplitude-modulated difference signals. Extensive simulations are conducted to validate the proposed estimation method in terms of estimation range and estimation root mean squared error (RMSE). Results show that, the proposed angle estimation method exhibits S-shaped curve characteristic under different angle errors, which is insensitive to channels and modulations. The proposed method obtains angle estimation RMSEs smaller than 0.18° for antenna element distance $d = 0.5$ m with 10 MHz OFDM signals. For both square- and absolute-value methods, a maximum degradation of 0.02° for angle estimation RMSEs is observed under Rician channels compared with the estimation under additive white Gaussian noise (AWGN) channels, whereas the absolute-value estimation outperforms the square-value estimation.

INDEX TERMS UAV target tracking, air-to-ground communication, single-channel monopulse tracking, OFDM signals, frequency selective fading channel, nonlinear detection.

I. INTRODUCTION

Unmanned aerial vehicles (UAVs) have tremendous potential in both military and civilian applications, including disaster search and rescue operations, surveillance, remote sensing, traffic monitoring, and goods transportations [1]–[3]. Position and orientation can greatly impact UAV link quality [4], formation control [5], path planning [6], and collision avoidance [7]. Targets tracking has found wide applications in radar, mobile satellite communication, and UAV remote sensing. Existing localization methods include global positioning system (GPS), beacon (or anchor) nodes and proximity-based localization, etc [8]. As we classified in [4], the unmanned aerial systems (UASs) differ one to each other for size and structure, like long-endurance UAVs of Predator and Global hawk, short-range small UAV of Scout, and very close-range one of Raven. UAV regulations in most countries usually require to equip with a GPS and an inertial measurement unit (IMU) for providing position information at any time [9]. When the GPS signal of conventional satellite-based systems is weak, ground-based positioning systems can be used in the context of indoor navigation [10]–[12], wireless emergency services and tactical military operations [13]. With the rapid development of wireless communication techniques, the communication signals available can be utilized and shared by UAV and ground station (GS) cooperatively to calculate the UAV location and tracking the moving target [14], [15].

The associate editor coordinating the review of this manuscript and approving it for publication was Di He.

A. UAV POSITIONING AND TRACKING

Generally, the airborne and ground stations have omnidirectional antennas or directional antennas for UAV communications [4]. Relatively large UAS often uses directional highly focused beams to achieve connectivity with more distinct systems. Directional antennas usually require node location information for beam pointing. UAV communication links can be broadly classified into two aspects namely, air-to-ground (A2G) communications and air-to-air (A2A) communications [16], [17]. In multi-UAV networks, the UAV position can be determined based on the ranging estimate from different transmitters, whereas the UAV position can also be calculated using ranging and angle information of single target.

The ranging-based localization methods in UAV communication systems infers location information taking advantage of a distance-dependent parameter in radio signals of multi-UAV networks [18]–[20]. The methods of received signal strength (RSS) [21], time of arrival (TOA) [22], [23], time difference of arrival (TDOA) [24], frequency difference of arrival (FDOA) [25], and angle of arrival (AOA) [26] are the most popular types of measurements. Localization schemes based on TOA or TDOA offer high precision, but this comes at the cost of a very complex process of accurate time synchronization among all users [27]. This localization requires multiple receivers or stations [28]–[30] and its performance is also highly related to the receiver-target deployment [31]. Ultra-wide bandwidth-based systems are commonly used in the localization community to obtain desirable localization performance and simple multipath mitigation without costly estimators but at the cost of a large bandwidth [32].

The other family member of self-positioning methods in UAV systems, monopulse tracking method is designed for tracking UAV target via a single array antenna on the ground station [33]. Conventional monopulse techniques usually require dedicated pulse to estimate the direction of a UAV target in A2G communication system. Additionally, linear modulations, continuous phase modulations, and direct-sequence spread-spectrum signals were also exploited to design monopulse tracking benefitting from their constant envelope characteristics [34], [35]. However, these signals with high rate suffer from multipath effect for A2G link with low elevation angles.

The airborne transmitter antenna is usually mounted on the underside of the aircraft fuselage and the GS is equipped with a tracking antenna. Active phased arrays, passive phased arrays and switched multiple-beam antennas are the approaches that enable electronically controlled beam steering and shaping. In order to achieve accurate UAV target pointing, the ground array antenna can provide pointing errors in elevation and azimuth related to the antenna beams of three tracking signals: the azimuth difference signal, the elevation difference signal and the sum signal. The monopulse tracking receivers can be implemented in single-channel, two-channel, and three-channel configurations based on amplitude-modulated difference signals [36]–[39]. The number of receiver channels of monopulse antennas is two for one-plane tracking and three for two-plane tracking [40]. More specifically, Shang *et al.* [38] proposed a phase calibration method for single-channel monopulse tracking (SCMT) systems using error voltage's convergence trajectory data with the aid of the curve fitting technique. Champion [39] designed a three-channel monopulse tracking receiver for upgrading tracking stations relying on commercial off-the-shelf equipment. Zheng *et al.* [41] provided a mathematical closed-form solution for identifying two targets based on a four-channel monopulse including both phase and amplitude monopulse measurement. Zhang *et al.* [42] suggested methods to localize multiple unresolved extended targets. Jardak *et al.* [43] divided the antenna array into multiple overlapping sets each of four antennas to detects two targets at generalized locations. Moreover, Nickel [44] overviewed the monopulse techniques and introduced the multi-dimensional generalized monopulse formula. For tracking requirement of communication satellites, Lacheta *et al.* designed a generic digital monopulse tracking receiver in [45], where the receiver was capable of being configured into single-channel and two-channel by adjusting the firmware. Conventional monopulse tracking systems are designed to operate with antenna arrays, whereas a multimode extractor for feed chain of monopulse tracking feed was presented at Ka band in [46]. In multi-mode monopulse tracking system, when the antenna receives an incident wave, the output of the communication signal is maximum and the antenna points directly toward a target signal source. When the boresight axis of the antenna feed is not in line with the target, higher order modes are activated in the circular waveguide.

B. MOTIVATION AND CONTRIBUTION

From the brief review above, we can find that monopulse techniques are well studied in both radar signal processing and target tracking literature. However, to the best of our knowledge, there is no literature studying monopulse tracking method utilizing the OFDM signals in UAV A2G communication systems. In the context of UAV A2G links with low elevation angles and multipath fading, OFDM is an effective solution to broadband communication resulting from its high spectral efficiency and robustness against frequency selective fading [47]–[50]. The amplitude-modulated difference signals in conventional UAV monopulse tracking system usually employ dedicated slave carrier pulses, spread-spectrum signals or single carrier linear modulations taking advantage of their approximately constant signal amplitudes, whereas the multicarrier OFDM signals with Gaussian-like distribution were not yet investigated to generate the amplitude-modulated difference signals for angle estimation. To fill this gap, this paper presents a novel SCMT method using the OFDM signals which was designed for high rate A2G telemetry and image data transmission, instead of using dedicated signals in UAV communication

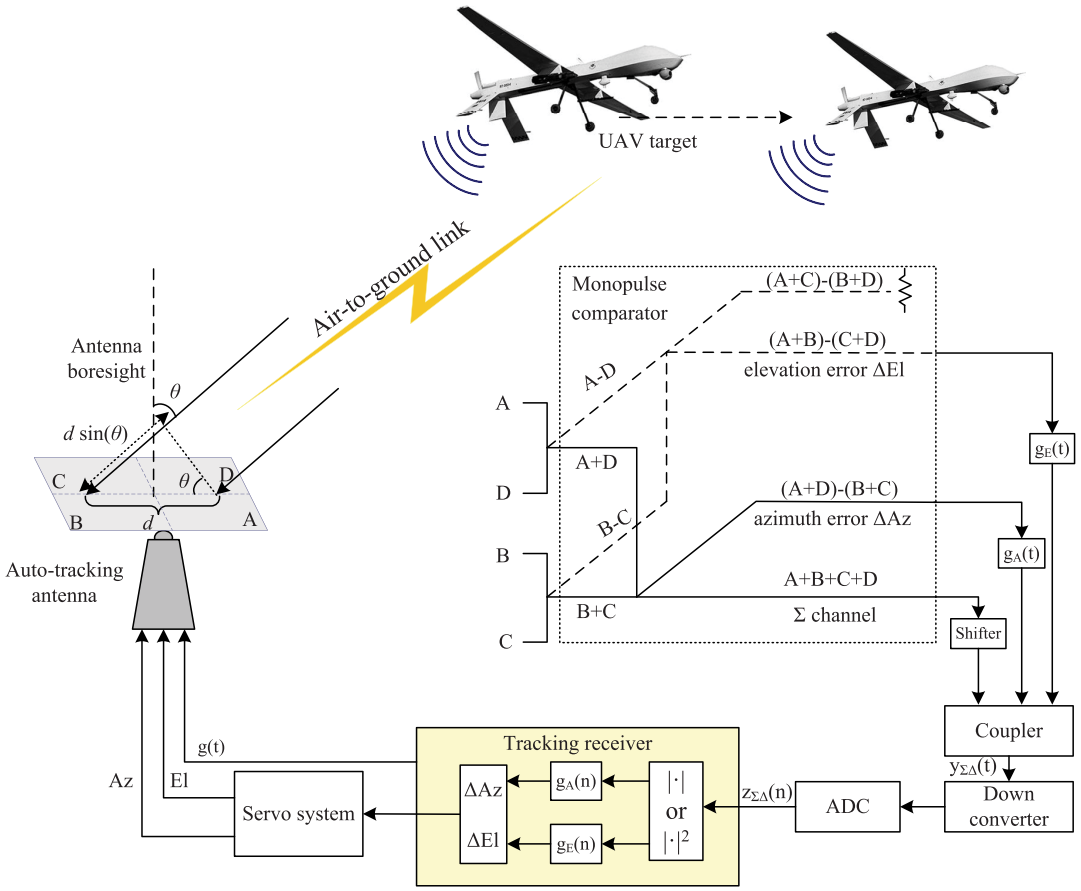

FIGURE 1. Target tracking architecture of monopulse technique exploiting UAV A2G communication signal.

and tracking system. The monopulse tracking system in the ground station operates relying on a planar antenna array for developing tracking signals.

The main contributions of this paper are summarized as follows:

- We propose an angle estimation method relying on the nonlinear detection for amplitude-modulated difference signals exploiting the OFDM communication signals at UAV ground station, and the angle estimation expressions are derived using two nonlinearity functions of square-value and absolute-value in SCMT receiver.
- We find that the proposed angle estimation method exhibits S-shaped curve characteristic under different angle errors, which is insensitive to channels and modulations. The estimation range relies on the distance between antenna elements. The S-curve of the absolute-value estimation outperforms that of the square-value estimation.
- Simulation results show that the angle estimation root mean squared errors (RMSEs) will get smaller for increasing sampling rates and signal-to-noise ratios (SNRs) of OFDM signal. A maximum degradation of 0.02° of the angle estimation RMSEs will be observed under Rician frequency selective channels compared with the estimation under additive white Gaussian noise (AWGN) channels for both square-value and absolute-value methods.

The remainder of this article is organized as follows. In Section II, we depict the diagram of the SCMT system in UAV A2G communication system. In Section III, we propose a novel SCMT angle estimation method using nonlinear detection of OFDM signals. Simulation results and analysis are presented in Section IV, followed by our conclusions in Section V.

II. SIGNAL MODEL

The monopulse tracking system consists of antenna-feed system, monopulse comparator, coupler, monopulse tracking receiver and antenna servo system, as shown in Fig. 1. Generally, two feeders A and B are separated by a distance d with parallel pointing directions for UAV target. The received signals are utilized to produce a phase difference $\Delta\varphi$ based on the angle-of-arrival θ, and we have $\Delta\varphi = 2\pi d \sin(\theta)/\lambda$, where λ is the wavelength of carrier frequency. This can be implemented with two antenna elements of the antenna array instead of two independent antennas. Monopulse comparator

generates the sum signal (Σ), azimuth error signal (ΔAz) and elevation error signal (ΔEl). For the two-channel mode, the azimuth error signal and the elevation error signal are combined [51], whereas for the single-channel mode, the azimuth error signal and the elevation error signal are multiplexed and coupled with the sum signal as the amplitude modulation signal [38]. The SCMT system with single receiver channel requires only one down converter and analog-to-digital converter (ADC) chain [45].

At the airborne transmitter in the UAV A2G link, the time domain OFDM signal $x(n)$ can be expressed as

$$x(n) = \frac{1}{\sqrt{N_s}} \sum_{k=0}^{N_s-1} X(k) e^{j2\pi kn/N_s}, \quad 0 \le n \le N_s - 1, \quad (1)$$

where N_s is the size of inverse fast Fourier transform (IFFT), and $X(k)$ represents the data sequence modulated on the k-th subcarrier with M-ary quadrature amplitude modulation (M-QAM) or M-ary phase shift keying (M-PSK). Through digital-to-analog converter (DAC) and power amplifier, the output of the transmitter is denoted as $x(t)$. Considering the A2G radio channel, the OFDM signal received at the ground station, $s(t)$, can be expressed as

$$s(t) = \int x(t-\tau)h(\tau)d\tau + w(t), \quad (2)$$

where $h(t)$ is the channel impulse response and $w(t)$ represents the zero-mean complex AWGN with zero mean and the variance of σ_w^2.

At the ground station, the signal arriving at antenna elements A, B, C and D in Fig. 1 can be written as

$$y_A(t) = A_m s(t) \sin(\omega t + \frac{\pi d}{\lambda} \sin\theta_A + \frac{\pi d}{\lambda} \sin\theta_E), \quad (3)$$

$$y_B(t) = A_m s(t) \sin(\omega t - \frac{\pi d}{\lambda} \sin\theta_A + \frac{\pi d}{\lambda} \sin\theta_E), \quad (4)$$

$$y_C(t) = A_m s(t) \sin(\omega t - \frac{\pi d}{\lambda} \sin\theta_A - \frac{\pi d}{\lambda} \sin\theta_E), \quad (5)$$

as well as

$$y_D(t) = A_m s(t) \sin(\omega t + \frac{\pi d}{\lambda} \sin\theta_A - \frac{\pi d}{\lambda} \sin\theta_E), \quad (6)$$

respectively, where A_m is the signal gain, ω represents the frequency, λ is the wavelength, and d denotes the distance between A (C) and B (D), or between A (B) and D (C). Moreover, θ_A and θ_E denote the angle of azimuth error and elevation error, respectively.

III. NONLINEARITY-BASED UAV TRACKING METHOD WITH OFDM SIGNALS

In this section, we commence with angle estimation based on square-value nonlinearity using OFDM signals received at tracking receiver. Then, we analyze the practical implementation approximation and propose an alternative method based on absolute-value nonlinearity.

A. SQUARE-VALUE-BASED ANGLE ESTIMATION

In the SCMT receiver, the sum signal and difference signals can be expressed as (7) – (9), as shown at the bottom of this page, where the difference slope μ is the scaling factor designed in monopulse antenna and it is assumed to be $\mu = 1$ here. In terms of small azimuth and elevation angle errors θ_A and θ_E, because of the approximation $\cos(\frac{\pi d}{\lambda}\sin\theta_A) \approx 1$ and $\sin(\frac{\pi d}{\lambda}\sin\theta_A) \approx \frac{\pi d}{\lambda}\theta_A$, we can rewrite (7) – (9) as (10) – (12).

$$y_\Sigma(t) \approx 4A_m s(t) \sin(\omega t), \quad (10)$$

$$y_{\Delta_A}(t) \approx 4A_m \mu s(t) \frac{\pi d}{\lambda} \theta_A \cos(\omega t), \quad (11)$$

$$y_{\Delta_E}(t) \approx 4A_m \mu s(t) \frac{\pi d}{\lambda} \theta_E \cos(\omega t). \quad (12)$$

These azimuth error (ΔAz) and elevation error (ΔEl) in Fig. 1 are multiplied with the azimuth/elevation scan (AES) pulses $g_A(t)$ and $g_E(t)$,

$$g_A(t) = \begin{cases} +1, & 0 < t \le \frac{T}{2}, \\ -1, & \frac{T}{2} < t \le T, \end{cases} \quad \text{and} \quad g_E(t) = g_A(t + \frac{T}{4}). \quad (13)$$

where T is the period of pulses.

The multiplied signals $y_{\Delta_A}(t)g_A(t)$ and $y_{\Delta_E}(t)g_E(t)$ are coupled with the sum signal through a $\pi/2$ phase shifter which aligns the sum signal $y_{\Sigma'}(t)$ in order to get the maximum signal at the output. The sum signal can be expressed as,

$$y_{\Sigma'}(t) = 4A_m s(t) \cos(\omega t). \quad (14)$$

The coupler output signal $y_{\Sigma\Delta}(t)$ of (15), as shown at the bottom of this page, is an amplitude modulation signal and the modulation index is proportional to the coupling factor G [45].

The amplitude modulation signal is down-converted and then is filtered with low-pass filter to the baseband digital sampling signal $z_{\Sigma\Delta}(n)$, where n is the sampling index.

$$y_\Sigma(t) = y_A(t) + y_B(t) + y_C(t) + y_D(t) = 4A_m s(t) \cos\left(\frac{\pi d}{\lambda}\sin\theta_A\right) \cos\left(\frac{\pi d}{\lambda}\sin\theta_E\right) \sin(\omega t), \quad (7)$$

$$y_{\Delta_A}(t) = y_A(t) - y_B(t) - y_C(t) + y_D(t) = 4A_m \mu s(t) \sin\left(\frac{\pi d}{\lambda}\sin\theta_A\right) \cos\left(\frac{\pi d}{\lambda}\sin\theta_E\right) \cos(\omega t), \quad (8)$$

$$y_{\Delta_E}(t) = y_A(t) + y_B(t) - y_C(t) - y_D(t) = 4A_m \mu s(t) \cos\left(\frac{\pi d}{\lambda}\sin\theta_A\right) \sin\left(\frac{\pi d}{\lambda}\sin\theta_E\right) \cos(\omega t), \quad (9)$$

The digital tracking receiver detects the sampling signal using the AES pulses $g_A(n)$ and $g_E(n)$. Thus, we obtain the envelope detection expressions $r_A(n)$ and $r_E(n)$ as follows,

$$r_A(n) = E\left\{g_A(n)\,|z_{\Sigma\Delta}(n)|^2\right\}, \tag{16}$$

$$r_E(n) = E\left\{g_E(n)\,|z_{\Sigma\Delta}(n)|^2\right\}, \tag{17}$$

where $E\{\cdot\}$ denotes the expectation. Then, $r_A(n)$ and $r_E(n)$ can be written as (18) and (19), as shown at the bottom of this page, respectively.

Bearing in mind that the expectations of pulses g_A, g_E in (13) can be given as

$$E\{g_A(n)g_E(n)\} = 0, \tag{20}$$

$$E\{g_A^2(n)\} = \{g_E^2(n)\} = 1, \tag{21}$$

we derive the $r_A(n)$, $r_E(n)$ in (16) – (17) as

$$r_A(n) = 16A_m^2 G\frac{\pi d}{\lambda}\mu\theta_A E\{|s(n)|^2\}, \tag{22}$$

$$r_E(n) = 16A_m^2 G\frac{\pi d}{\lambda}\mu\theta_E E\{|s(n)|^2\}. \tag{23}$$

Therefore, the proposed angle estimations $\hat{\theta}_A$, $\hat{\theta}_E$ relying on OFDM signals $s(n)$ can be formulated as

$$\hat{\theta}_A = \frac{r_A(n)\lambda}{16A_m^2\mu G\pi d E\{|s(n)|^2\}}, \tag{24}$$

and

$$\hat{\theta}_E = \frac{r_E(n)\lambda}{16A_m^2\mu G\pi d E\{|s(n)|^2\}}. \tag{25}$$

Define the secondary moment $M_2 \triangleq E\{|z_{\Sigma\Delta}(n)|^2\}$, we can calculate M_2 as (26), as shown at the bottom of the next page, where we have $(G\pi d\mu\theta/\lambda)^2 \ll 1$ for small value of $\theta = \sqrt{\theta_A^2 + \theta_E^2}$. Hence, by neglecting $(G\pi d\mu\theta/\lambda)^2$ in (26), we have the approximation

$$M_2 \approx 8A_m^2 E\{|s(n)|^2\}. \tag{27}$$

Thus, we achieve the updated angle estimation $\hat{\theta}_A$, $\hat{\theta}_E$ as,

$$\hat{\theta}_A = \frac{r_A(n)\lambda}{2\mu G\pi d M_2}, \tag{28}$$

and

$$\hat{\theta}_E = \frac{r_E(n)\lambda}{2\mu G\pi d M_2}, \tag{29}$$

which are expressed as normalization by OFDM signal power $E\{|s(n)|^2\}$.

For conventional UAV tracking receiver in low rate data transmission system using direct-sequence spread-spectrum, the signal $s(n)$ is replaced with the constant envelope spread-spectrum sequence $c(n')$ and the fact that $|c(n')| = 1$ will eliminate the influence of signal amplitude. However, OFDM signal for high rate data transmission will benefit from its robustness against A2G multipath fading channel and it is capable of achieving desired angle estimation by our proposed algorithm.

B. IMPLEMENTATION AND ALTERNATIVE ESTIMATION WITH ABSOLUTE-VALUE

Considering the practical implementation, we can approximate the expectation $r_A(n)$ (16), $r_E(n)$ (17) over a period of T in (13) as the accumulation,

$$r_A(n) \approx \sum_T g_A(n)\,|z_{\Sigma\Delta}(n)|^2\,, \tag{30}$$

$$r_E(n) \approx \sum_T g_E(n)\,|z_{\Sigma\Delta}(n)|^2\,. \tag{31}$$

Similarly, the secondary moment M_2 is approximated as the accumulation,

$$M_2 \approx \sum_T |z_{\Sigma\Delta}(n)|^2\,. \tag{32}$$

Accordingly, we approximate the angle estimations (28) and (29) relying on the signal power as $\hat{\theta}'_A$, $\hat{\theta}'_E$,

$$\hat{\theta}'_A \approx \frac{\lambda\sum_T g_A(n)\,|z_{\Sigma\Delta}(n)|^2}{2\mu G\pi d\sum_T |z_{\Sigma\Delta}(n)|^2}, \tag{33}$$

and

$$\hat{\theta}'_E \approx \frac{\lambda\sum_T g_E(n)\,|z_{\Sigma\Delta}(n)|^2}{2\mu G\pi d\sum_T |z_{\Sigma\Delta}(n)|^2}. \tag{34}$$

which are expressed as normalization by OFDM signal power $\Sigma_T\,|z_{\Sigma\Delta}(n)|^2$ over a period of T.

Alternative Estimation with Absolute-Value. After investigating the estimations $\hat{\theta}_A$, $\hat{\theta}_E$ above, we hereby present alternative angle estimation solutions (35) – (36) using absolute-value instead of the square-value in (16) and (17).

$$r_{A1}(n) = E\Big\{g_A(n)\,|z_{\Sigma\Delta}(n)|\,\Big\}, \tag{35}$$

$$y_{\Sigma\Delta}(t) = y_{\Sigma'}(t) + G\left[y_{\Delta_A}(t)g_A(t) + y_{\Delta_E}(t)g_E(t)\right] = 4A_m s(t)\cos(\omega t)\left[1 + G\left(\frac{\pi d}{\lambda}\mu\theta_A g_A(t) + \frac{\pi d}{\lambda}\mu\theta_E g_E(t)\right)\right]. \tag{15}$$

$$r_A(n) = 8A_m^2 E\left\{g_A(n)|s(n)|^2\left[1 + G\frac{\pi d}{\lambda}\mu(\theta_A g_A(n) + \theta_E g_E(n))\right]^2\right\}, \tag{18}$$

$$r_E(n) = 8A_m^2 E\left\{g_E(n)|s(n)|^2\left[1 + G\frac{\pi d}{\lambda}\mu(\theta_A g_A(n) + \theta_E g_E(n))\right]^2\right\}. \tag{19}$$

$$r_{E1}(n) = E\left\{g_E(n)\,|z_{\Sigma\Delta}(n)|\right\}. \tag{36}$$

Define the first moment $M_1 = E\{|z_{\Sigma\Delta}(n)|\}$. we then directly derive the angle estimation expressions as,

$$\hat{\theta}_{A1} = \frac{r_{A1}(n)\lambda}{\mu G\pi d M_1}, \quad \hat{\theta}_{E1} = \frac{r_{E1}(n)\lambda}{\mu G\pi d M_1}. \tag{37}$$

We approximate the angle estimations $\hat{\theta}_{A1}$, $\hat{\theta}_{E1}$ as (38) and (39) relying on normalization by the absolute value of OFDM signal $\Sigma_T\,|z_{\Sigma\Delta}(n)|$, i.e.

$$\hat{\theta}'_{A1} \approx \frac{\lambda \sum_T g_A(n)\,|z_{\Sigma\Delta}(n)|}{\mu G\pi d \sum_T |z_{\Sigma\Delta}(n)|}, \tag{38}$$

and

$$\hat{\theta}'_{E1} \approx \frac{\lambda \sum_T g_E(n)\,|z_{\Sigma\Delta}(n)|}{\mu G\pi d \sum_T |z_{\Sigma\Delta}(n)|}. \tag{39}$$

It is very challenging to derive the theoretical performance of (33)–(39) for multicarrier OFDM signals. In the following section, we will evaluate the angle estimation performance of the proposed method through extensive simulations.

IV. RESULTS AND DISCUSSIONS

In this section, we will evaluate our proposed method in terms of angle estimation range as well as the estimation RMSE performance using OFDM signals in both AWGN and frequency-selective channel.

A. SIMULATION SETTING

Following the target tracking architecture described in Fig. 1, we set the simulation frequency for monopulse tracking antenna to be L-band (1.5 GHz) and the antenna element distance is $d = 0.5$ m or 0.9 m with coupling factor $G = 1/4$, difference slope $\mu = 1$ and AES pulse period $T = 1$ ms. Our OFDM system has an IFFT/FFT length of $N_s = 1024$, where the edge IFFT bins are not used. The spacing between two subcarriers is 10 kHz with each subcarrier mapped by M-QAM. The sampling rate of OFDM signals is 10.24 MHz. The Rician fading channel used is modelled as 10 paths with path delays τ_n of $n = 1, 2, \ldots, 10$ samples, exponentially decaying path gains of $e^{-\tau_n/3}$ and K factor of 10 dB [52]. The parameters are summarized in Table 1.

Following the setting above, we express the proposed angle estimations of (33) and (34) as

$$\hat{\theta}'_A = \frac{2\lambda \sum_T g_A(n)\,|z_{\Sigma\Delta}(n)|^2}{\pi d \sum_T |z_{\Sigma\Delta}(n)|^2}, \tag{40}$$

and

$$\hat{\theta}'_E = \frac{2\lambda \sum_T g_E(n)\,|z_{\Sigma\Delta}(n)|^2}{\pi d \sum_T |z_{\Sigma\Delta}(n)|^2}. \tag{41}$$

TABLE 1. Parameters setting in simulations.

Parameter	Values
Antenna	monopulse
Frequency	1.5 GHz
Element distance, d	0.5 m, 0.9 m
Coupling factor, G	1/4
Slope, μ	1
Pulse period, T	1 ms
N_s of OFDM	1024
OFDM sampling rate	5.12, 10.24, 20.48 MHz
Modulation	4QAM, 16QAM
Channel	Rician, AWGN
Rice factor, K	10 dB

The corresponding absolute-value estimation in (38) and (39) can be expressed as,

$$\hat{\theta}'_{A1} = \frac{4\lambda \sum_T g_A(n)\,|z_{\Sigma\Delta}(n)|}{\pi d \sum_T |z_{\Sigma\Delta}(n)|}, \tag{42}$$

and

$$\hat{\theta}'_{E1} = \frac{4\lambda \sum_T g_E(n)\,|z_{\Sigma\Delta}(n)|}{\pi d \sum_T |z_{\Sigma\Delta}(n)|}. \tag{43}$$

To the best of our knowledge, there is no literature studying monopulse tracking taking advantage of OFDM signals. Therefore, we present our simulation results in the framework of angle estimation range and RMSE performance for our proposed methods (40) – (43) without comparisons with other methods.

B. ANGLE ESTIMATION RANGE

Figure 2 shows the angle estimation performance of proposed method versus different azimuth or elevation angle errors with 4-QAM modulation and antenna element distance $d = 0.5$ m, 0.9 m. The angle error estimation results can be characterized by an 'S-shape' curve, which is independent of channels and modulations. From (40) – (43), we can find that the S-curve will only rely on wavelength λ, antenna element distance d and receiving OFDM signal. The zero-crossing point angle errors of the S-curve are the equilibrium states of auto-tracking system. The zero-crossing points $\pm 6.4°$, $\pm 11.5°$ in Fig. 2 are the maximum acquisition angle values for the auto-tracking antenna using proposed method. We can find that the maximum azimuth or elevation angle estimation ϕ decreases for increasing d, i.e. for $d = 0.5$ m, 0.9 m, $\phi = \pm 11.5°, \pm 6.4°$, respectively. The azimuth (or elevation) angle estimation S-curve can be defined as the average estimator output in the range of $|\theta_e| \le |\phi|$, i.e.,

$$S(\theta_e) = E[\hat{\theta}_A(n) | \forall n : |\theta_e| \le |\phi|]. \tag{44}$$

The 3 dB beamwidths for antenna can be approximated as $2\theta_h \approx 70° \times \lambda/D_a$ where D_a is antenna equivalent

$$M_2 = 8A_m^2 E\left\{|s(n)|^2\left[1 + G\frac{\pi d}{\lambda}\mu(\theta_A g_A(n) + \theta_E g_E(n))\right]^2\right\} = 8A_m^2 E\left\{|s(n)|^2\left[1 + \left(\frac{G\pi d\mu\theta}{\lambda}\right)^2\right]\right\}, \tag{26}$$

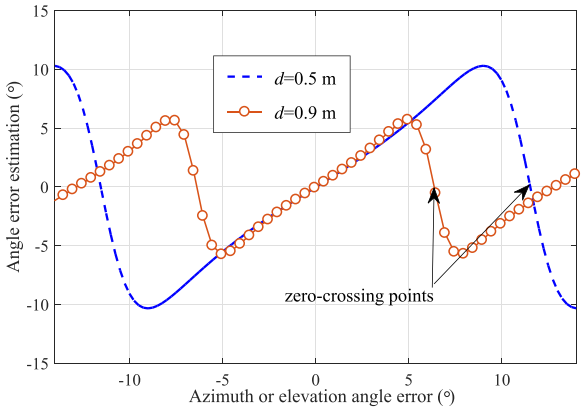

FIGURE 2. Angle error estimation output S-curve for proposed method (40) or (41) versus different azimuth or elevation angle errors θ_e, $d = 0.5$ m, 0.9 m.

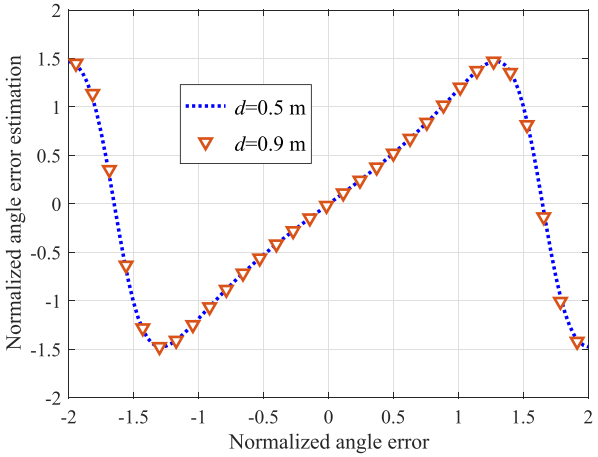

FIGURE 3. Normalized angle estimation output S-curve for proposed method (45), $d = 0.5$ m, 0.9 m.

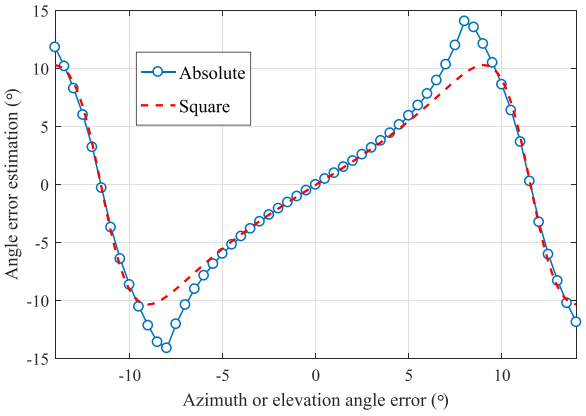

FIGURE 4. Angle estimation performance for proposed absolute-value method (42) or (43) versus different azimuth or elevation errors θ_e, $d = 0.5$ m.

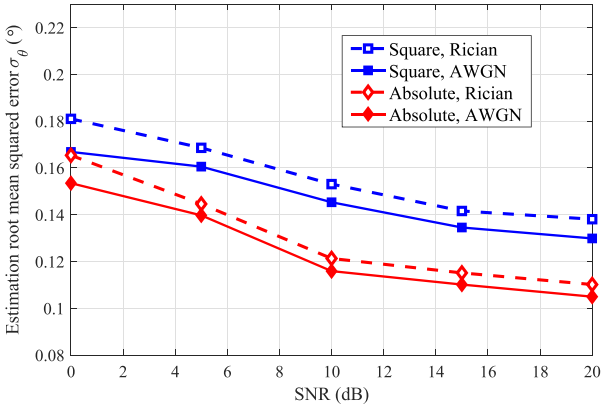

FIGURE 5. Estimation RMSE performance versus SNR under Rician channel and AWGN channel for proposed square- and absolute-value methods, $d = 0.5$ m.

aperture [53]. Our monopulse array antenna has $D_a = 2d$. Thus we have $2\theta_h \approx 14°$ and 7.7° for $d = 0.5$ m, 0.9 m, respectively. To further analyze the estimation performance, we then normalize the angle estimation $\hat{\theta}_A$ and $\hat{\theta}_E$ by θ_h, and get the normalized estimation values, $\bar{\theta}_A$ and $\bar{\theta}_E$, i.e.

$$\bar{\theta}_A = \frac{\hat{\theta}_A}{\theta_h}, \quad \bar{\theta}_E = \frac{\hat{\theta}_E}{\theta_h}. \tag{45}$$

Simulation results for normalized estimations (45) are presented in Fig. 3, where the estimation S-curves for $d = 0.5$ m, 0.9 m have identical characteristic. The angle estimation range ϕ is proportional to θ_h and their relationship can be approximately expressed as $|\phi| \approx 1.65\,\theta_h$.

We also studied the estimation performance of the proposed absolute-value method (42), (43) for $d = 0.5$ m, as shown in Fig. 4. Results show that the absolute-value method exhibits larger estimation values than the square-value method for the same angle errors. The proposed SCMT angle estimation method will feed the angle estimation results to auto-tracking antenna servo system and construct a closed loop for tracking target. This absolute-value method will enhance the auto-tracking antenna sensitivity to changing angle errors of UAV target. We will next examine the proposed method from the view of the RMSE performance.

C. ANGLE ESTIMATION RMSE

The angle estimation RMSEs under both frequency selective fading channels and AWGN channels are given in Fig. 5, Fig. 6 for antenna element distance $d = 0.5$ m, 0.9 m, respectively. The estimation RMSEs under our Rician channels show degradation of 0.01° – 0.02° compared with the estimation under AWGN channels for both square-value and absolute-value methods. Under AWGN channels, the proposed square-value method exhibits robust RMSE performance with $\sigma_\theta < 0.17°$, 0.11°, respectively, within the SNR region from 0 dB to 20 dB. In the case of the absolute-value method, we can find that it has decreasing RMSEs, i.e. $\sigma_\theta < 0.16°$, 0.09° for $d = 0.5$ m, 0.9 m, respectively.

The absolute-value estimation outperforms the square-value estimation because the high-order moment of baseband signal $\sum_T |z_{\Sigma\Delta}(n)|^2$ in (40) and (41) enlarges influence of

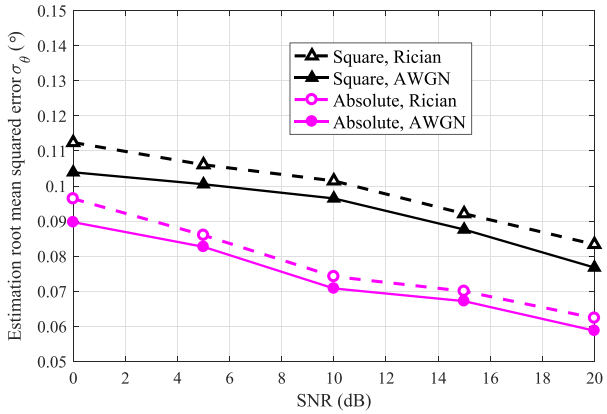

FIGURE 6. Estimation RMSE performance versus SNR under Rician channel and AWGN channel for proposed square- and absolute-value methods, $d = 0.9$ m.

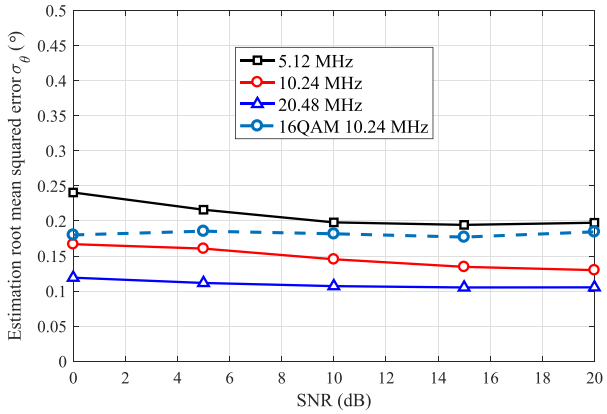

FIGURE 7. Estimation RMSE performance of proposed square-value methods in the context of different OFDM sampling rates under AWGN channels, $d = 0.5$ m.

noise and interference in $z_{\Sigma\Delta}(n)$ compared with the low-order one $\sum_T |z_{\Sigma\Delta}(n)|$ in (42) and (43).

Figure 7 presents the estimation RMSEs of the proposed square-value method under AWGN channels with different OFDM sampling rates of 5.12 MHz, 10.24 MHz and 20.48 MHz for $d = 0.5$ m. We can find that, compared with 10.24 MHz, the RMSEs for 5.12 MHz degrade by about 0.07°, whereas the RMSEs for 20.48 MHz outperform the case of 10.24 MHz by about 0.07°. For higher-order mapping scheme, i.e. 16-QAM, with sampling rate 10.24 MHz, a maximum RMSE degradation of 0.05° is observed as shown by the dot-line in Fig. 7, although their S-curves in Fig. 2 have the same characteristics. Not that, the rich multipath scenario of UAV air-to-ground communication with high mobility and low elevation imposes restrictions on employing high-order mapping schemes. Therefore, 10 MHz OFDM signals with 4-QAM mapping and square-value estimation are recommended for practical implementation in UAV communication system, whereas antenna element distance d and aperture D_a depend on the requirement of link budget and ground station coverage area.

V. CONCLUSION

In this paper, we construct an SCMT receiver architecture exploiting OFDM signals in UAV A2G communication system and then propose an angle estimation method using square-value and absolute-value nonlinearities of amplitude-modulated OFDM difference signals. Extensive simulations are conducted for evaluating the performance of our proposed angle estimation method in terms of the estimation range and RMSE. Results show that, the proposed angle estimation method has S-curve characteristic which is insensitive to channels and modulations. The estimation RMSEs improve with increasing OFDM signal sampling rates and SNRs, whereas a maximum degradation of 0.02° is observed under Rician channels compared with the estimation under AWGN channels. The estimation results of the proposed SCMT angle estimation method will finally be fed to auto-tracking antenna and a closed loop is constructed for tracking UAV target.

REFERENCES

[1] K. Namuduri, S. Chaumette, J. H. Kim, and J. P. Sterbenz, *UAV Networks and Communications*. Cambridge, U.K.: Cambridge Univ. Press, 2018.
[2] J. Wang, C. Jiang, Z. Han, Y. Ren, R. G. Maunder, and L. Hanzo, "Taking drones to the next level: Cooperative distributed unmanned-aerial-vehicular networks for small and mini drones," *IEEE Veh. Technol. Mag.*, vol. 12, no. 3, pp. 73–82, Sep. 2017.
[3] S. Hayat, E. Yanmaz, and R. Muzaffar, "Survey on unmanned aerial vehicle networks for civil applications: A communications viewpoint," *IEEE Commun. Surveys Tuts.*, vol. 18, no. 4, pp. 2624–2661, 4th Quart., 2016.
[4] C. Yan, L. Fu, J. Zhang, and J. Wang, "A comprehensive survey on UAV communication channel modeling," *IEEE Access*, vol. 7, pp. 107769–107792, 2019.
[5] J. Yan, H. Zhao, X. Luo, C. Chen, and X. Guan, "RSSI-based heading control for robust long-range aerial communication in UAV networks," *IEEE Internet Things J.*, vol. 6, no. 2, pp. 1675–1689, Apr. 2019.
[6] Z. Wu, J. Li, J. Zuo, and S. Li, "Path planning of UAVs based on collision probability and Kalman filter," *IEEE Access*, vol. 6, pp. 34237–34245, 2018.
[7] Y. Wang, T. Sun, G. Rao, and D. Li, "Formation tracking in sparse airborne networks," *IEEE J. Sel. Areas Commun.*, vol. 36, no. 9, pp. 2000–2014, Sep. 2018.
[8] C. Yan, L. Fu, M. Chen, and D. Jiao, "FIR-based ranging method for OFDM communication systems of networking UAVs," in *Proc. IEEE/CIC Int. Conf. Commun. China*, Beijing, China, Aug. 2018, pp. 631–635.
[9] C. Stöcker, R. Bennett, F. Nex, M. Gerke, and J. Zevenbergen, "Review of the current state of UAV regulations," *Remote Sens.*, vol. 9, no. 5, p. 459, May 2017.
[10] D. He, T. Bouras, X. Chen, W. Yu, Y. Zhang, and Y. Yang, "3-D spatial spectrum fusion indoor localization algorithm based on CSI-UCA smoothing technique," *IEEE Access*, vol. 6, pp. 59575–59588, 2018.
[11] Z. Tang, D. He, S. Arai, and D. Zou, "Positioning-aided scheme for image sensor communication using single-view geometry," in *Proc. IEEE Int. Symp. Circuits Syst. (ISCAS)*, May 2019, pp. 1–5.
[12] D. He, X. Chen, D. Zou, L. Pei, and L. Jiang, "A novel wireless positioning approach based on distributed stochastic-resonance-enhanced power spectrum fusion technique," in *Proc. IEEE Int. Symp. Circuits Syst. (ISCAS)*, May 2019, pp. 1–5.
[13] S. M. Sherman, *Monopulse Principles and Techniques*. Norwood, MA, USA: Artech House, 1984.
[14] Y. Qu and Y. Zhang, "Cooperative localization against GPS signal loss in multiple UAVs flight," *J. Syst. Eng. Electron.*, vol. 22, no. 1, pp. 103–112, 2011.
[15] M. Hamaoui, "Non-iterative MDS method for collaborative network localization with sparse range and pointing measurements," *IEEE Trans. Signal Process.*, vol. 67, no. 3, pp. 568–578, Feb. 2019.

[16] W. Khawaja, I. Guvenc, D. W. Matolak, U.-C. Fiebig, and N. Schneckenburger, "A survey of air-to-ground propagation channel modeling for unmanned aerial vehicles," *IEEE Commun. Surveys Tuts.*, vol. 21, no. 3, pp. 2361–2391, 3rd Quart., 2019.
[17] J. Zhang, T. Chen, S. Zhong, J. Wang, W. Zhang, X. Zuo, R. G. Maunder, and L. Hanzo, "Aeronautical ad hoc networking for the Internet-above-the-clouds," *Proc. IEEE*, vol. 107, no. 5, pp. 868–911, May 2019.
[18] C. Yan, J. Wang, L. Fu, C. Jiang, M. Chen, and Y. Ren, "Timing synchronization and ranging in networked UAV-aided OFDM systems," *J. Commun. Inf. Netw.*, vol. 3, no. 4, pp. 45–54, 2018.
[19] X. Pan, S. Liu, and S. Yan, "Nonlinearity-based ranging technique in SC-FDE communication system with oversampled signals," *IEEE Access*, vol. 7, pp. 49632–49640, 2019.
[20] X. Pan, C. Xiang, S. Liu, and S. Yan, "Low-complexity time-domain ranging algorithm with FMCW sensors," *Sensors*, vol. 19, no. 14, p. 3176, 2019.
[21] G. Li, E. Geng, Z. Ye, Y. Xu, J. Lin, and Y. Pang, "Indoor positioning algorithm based on the improved RSSI distance model," *Sensors*, vol. 18, no. 9, p. 2820, Aug. 2018.
[22] I. Guvenc and C.-C. Chong, "A survey on TOA based wireless localization and NLOS mitigation techniques," *IEEE Commun. Surveys Tuts.*, vol. 11, no. 3, pp. 107–124, 3rd Quart., 2009.
[23] W. Yuan, N. Wu, Q. Guo, X. Huang, Y. Li, and L. Hanzo, "TOA based passive localization constructed over factor graphs: A unified framework," *IEEE Trans. Commun.*, to be published.
[24] H. Ni, G. Ren, and Y. Chang, "A TDOA location scheme in OFDM based WMANs," *IEEE Trans. Consum. Electron.*, vol. 54, no. 3, pp. 1017–1021, Aug. 2008.
[25] K. C. Ho and W. Xu, "An accurate algebraic solution for moving source location using TDOA and FDOA measurements," *IEEE Trans. Signal Process.*, vol. 52, no. 9, pp. 2453–2463, Sep. 2004.
[26] S. Tomic, M. Beko, R. Dinis, and L. Bernardo, "On target localization using combined RSS and AoA measurements," *Sensors*, vol. 18, no. 4, p. 1266, 2018.
[27] Y. Xiong, N. Wu, Y. Shen, and M. Z. Win, "Cooperative network synchronization: Asymptotic analysis," *IEEE Trans. Signal Process.*, vol. 66, no. 3, pp. 757–772, Feb. 2018.
[28] L. Dai, Z. Wang, C. Pan, and S. Chen, "Wireless positioning using TDS-OFDM signals in single-frequency networks," *IEEE Trans. Broadcast.*, vol. 58, no. 2, pp. 236–246, Jun. 2012.
[29] W. Yuan, N. Wu, B. Etzlinger, Y. Li, C. Yan, and L. Hanzo, "Expectation–maximization-based passive localization relying on asynchronous receivers: Centralized versus distributed implementations," *IEEE Trans. Commun.*, vol. 67, no. 1, pp. 668–681, Jan. 2019.
[30] W. Yuan, N. Wu, B. Etzlinger, H. Wang, and J. Kuang, "Cooperative joint localization and clock synchronization based on Gaussian message passing in asynchronous wireless networks," *IEEE Trans. Veh. Technol.*, vol. 65, no. 9, pp. 7258–7273, Sep. 2016.
[31] W. Wang, P. Bai, Y. Zhou, X. Liang, and Y. Wang, "Optimal configuration analysis of AOA localization and optimal heading angles generation method for UAV swarms," *IEEE Access*, vol. 7, pp. 70117–70129, 2019.
[32] E. Staudinger, S. Zhang, and A. Dammann, "Cramer-rao lower bound for round-trip delay ranging with subcarrier-interleaved OFDMA," *IEEE Trans. Aerosp. Electron. Syst.*, vol. 52, no. 6, pp. 2961–2972, Dec. 2016.
[33] S. Jenvey, J. Gustafsson, and F. Henriksson, "A portable monopulse tracking antenna for UAV communications," in *Proc. Int. Unmanned Air Veh. Syst. Conf.*, Bristol, U.K., Apr. 2007, pp. 1–7.
[34] U. Nickel, "Monopulse estimation with adaptive arrays," *IEE Proc. F Radar Signal Process.*, vol. 140, no. 5, pp. 303–308, Oct. 1993.
[35] W. D. Blair and M. Brandt-Pearce, "Unresolved Rayleigh target detection using monopulse measurements," *IEEE Trans. Aerosp. Electron. Syst.*, vol. 34, no. 2, pp. 543–552, Apr. 1998.
[36] B. R. Mahafza, *Radar Systems Analysis and Design Using MATLAB*. Boca Raton, FL, USA: CRC Press, 2000.
[37] R. R. Yaminy, "A two-channel monopulse telemetry and tracking antenna feed," in *Proc. Int. Telemetering Conf.*, 1968, pp. 1–13.
[38] Y.-H. Shang, H. Luo, and F.-X. Yu, "A phase calibration method for single channel monopulse tracking systems based on curve fitting technique," in *Proc. 2nd Int. Conf. Instrum., Meas., Comput., Commun. Control (IMCCC)*, Harbin, China, Dec. 2012, pp. 577–580.
[39] J. Champion, "A 3-channel monopulse tracking receiver system using commercial off-the-shelf equipment," in *Proc. Int. Telemetering Conf.*, 1998, pp. 1–8.
[40] H. Wang, D. Fang, and M. Li, "A single-channel microstrip electronic tracking antenna array with time sequence phase weighting on sub-array," *IEEE Trans. Microw. Theory Techn.*, vol. 58, no. 2, pp. 253–258, Feb. 2010.
[41] Y. Zheng, S.-M. Tseng, and K.-B. Yu, "Closed-form four-channel monopulse two-target resolution," *IEEE Trans. Aerosp. Electron. Syst.*, vol. 39, no. 3, pp. 1083–1089, Jul. 2003.
[42] X. Zhang, P. Willett, and Y. Bar-Shalom, "Detection and localization of multiple unresolved extended targets via monopulse radar signal processing," *IEEE Trans. Aerosp. Electron. Syst.*, vol. 45, no. 2, pp. 455–472, Apr. 2009.
[43] S. Jardak, S. Ahmed, and M.-S. Alouini, "Generalised two target localisation using passive monopulse radar," *IET Radar, Sonar Navigat.*, vol. 11, no. 6, pp. 932–936, Jun. 2017.
[44] U. Nickel, "Overview of generalized monopulse estimation," *IEEE Aerosp. Electron. Syst. Mag.*, vol. 21, no. 6, pp. 27–56, Jun. 2006.
[45] S. Lacheta, P. K. Gupta, and J. K. Hota, "Generic digital monopulse tracking receiver for advanced communication satellites," in *Proc. IEEE Int. Conf. Electron., Comput. Commun. Technol. (CONECCT)*, Bangalore, India, Jul. 2015, pp. 1–5.
[46] A. K. Pandey, "Design of multimode tracking system for earth station antenna," in *Proc. Asia–Pacific Microw. Conf. (APMC)*, New Delhi, India, Dec. 2016, pp. 1–4.
[47] R. Jain and F. Templin, "Requirements, challenges and analysis of alternatives for wireless datalinks for unmanned aircraft systems," *IEEE J. Sel. Areas Commun.*, vol. 30, no. 5, pp. 852–860, Jun. 2012.
[48] M. C. Erturk, J. Haque, W. A. Moreno, and H. Arslan, "Doppler mitigation in OFDM-based aeronautical communications," *IEEE Trans. Aerosp. Electron. Syst.*, vol. 50, no. 1, pp. 120–129, Jan. 2014.
[49] J. Zhang, X. Mu, E. Chen, and S. Yang, "Decision-directed channel estimation based on iterative linear minimum mean square error for orthogonal frequency division multiplexing systems," *IET Commun.*, vol. 3, no. 7, pp. 1136–1143, Jul. 2009.
[50] J. Zhang, L. Hanzo, and X. Mu, "Joint decision-directed channel and noise-variance estimation for MIMO OFDM/SDMA systems based on expectation-conditional maximization," *IEEE Trans. Veh. Technol.*, vol. 60, no. 5, pp. 2139–2151, Jun. 2011.
[51] P. K. Gupta, R. Vaghela, K. A. Bhatt, and S. S. Valdiya, "Two-channel monopulse tracking receiver for onboard antenna tracking system," in *Proc. Int. Conf. Commun., Inf. Comput. Technol. (ICCICT)*, Mumbai, India, Oct. 2012, pp. 1–6.
[52] H. Minn, M. Zeng, and V. K. Bhargava, "On timing offset estimation for OFDM systems," *IEEE Commun. Lett.*, vol. 4, no. 7, pp. 242–244, Jul. 2000.
[53] E. Tuncer and B. Friedlander, *Classical and Modern Direction-of-Arrival Estimation*. New York, NY, USA: Academic, 2009.

XI PAN received the B.S., M.S., and Ph.D. degrees from the Beijing Institute of Technology, Beijing, China, in 1999, 2002, and 2007, respectively. She was a Visiting Scholar with the College of Engineering and Computer Science, Australian National University, from 2011 to 2012. She is currently an Associate Professor with the School of Mechatronical Engineering, Beijing Institute of Technology. She has been involved in a range of research projects, including four projects of NSFC, three Defense Key Laboratory funds, and two Advance Research Programs. She holds more than ten patents. Her current research interests include target tracking and ranging technique, and short range radar signal processing.

CHAOXING YAN received the Ph.D. degree in communication and information system from the Beijing Institute of Technology, China, in 2012. Since 2012, he has been with the Beijing Research Institute of Telemetry, where he is currently a Senior Engineer and an Associate Project Manager. In 2017, he was a Visiting Scholar with the Next-Generation Wireless Group, School of Electronics and Computer Science, University of Southampton, U.K., chaired by the Prof. L. Hanzo. His current research interests include wireless communication and networking techniques in terrestrial networks, UAV datalinks, and satellite and space communication networks. He was selected for the Youth Outstanding Talent Support Program of the China Aerospace Science and Technology Corporation (CASC), in 2019. He is the author of several scientific articles and the holder of over 30 patents. He serves as the Session Chair of IEEE/CIC ICCC 2018 and a Reviewer of several IEEE journals.

JIANKANG ZHANG received the B.Sc. degree in mathematics and applied mathematics from the Beijing University of Posts and Telecommunications, in 2006, and the Ph.D. degree in communication and information systems from Zhengzhou University, in 2012. He was a Lecturer, from 2012 to 2013, and an Associate Professor, from 2013 to 2014, with the School of Information Engineering, Zhengzhou University. From 2009 to 2011, he was a Visiting Ph.D. Student with the School of Electronics and Computer Science, University of Southampton, U.K. From 2013 to 2014, he was a Postdoctoral Researcher with McGill University, Canada. He is currently a Senior Research Fellow with the University of Southampton. His current research interests include wireless communications and signal processing, aeronautical communications, and broadband communications. Dr. Zhang was a recipient of a number of academic awards, including the Excellent Doctoral Dissertation of Henan Province, China, and the Youth Science and Technology Award of Henan Province, China. He serves as an Associate Editor of IEEE Access and a Guest Editor of a special issue on *EURASIP Journal on Advances in Signal Processing*.